FOREX Publication
Open Access | Rapid and quality publishing

International Journal of
Electrical and Electronics Research (IJEER)
Research Article | Volume 14, Issue 02| Pages 381-388 | e-ISSN: 2347-470X

Design and Realization of Circular Polarized Dual Band Planar Antenna using Metamaterial Techniques for Wireless Communications

Potnuru Narayanarao[1], Karunakar Godi[2]

[1]*Department of ECE, Aditya Institute of Technology and Management, Tekkali, AP-532201, India; narayana1student@gmail.com*
[2]*Department of ECE, GITAM (Deemed to be University), Visakhapatnam, AP-530045, India; kgodi@gitam.edu*

***Correspondence:** *Potnuru Narayanarao, narayana1student@gmail.com*

ABSTRACT– This work introduces a novel dual-band circular polarized (CP) microstrip patch antenna for wireless communications. The antenna features a square patch with corner truncated and an etched rectangular slot for circular polarization. The geometric modifications are mainly to control resonating frequencies, bandwidth and to optimize the axial ratio (AR) at the resonating frequencies. The proposed dual-band CP metamaterial antenna is designed to function within the wireless frequency ranges i.e., 2.28-2.48 GHz and 4.48-4.64 GHz with a measured gains of 2.62 dBi and 2.8 dBi at 2.4 as well as 4.5 GHz respectively. The CP is achieved using truncated corners at opposite sides and a slot in the square patch to improve the AR bandwidth. The dimensions of the proposed dual band antenna are 50 × 50 × 1.6 mm³.The antenna is realized using a low-cost FR-4 laminate with a ε_r of 4.4 and a tanδ of 0.02. The experimental performance of modeled antenna closely matches with the simulation results and confirms the effectiveness of the design methodology. Comparative analysis further indicates that the proposed antenna achieves higher gain and occupies less physical area relative to similar designs reported in recent literature.

Keywords: Dual band, Metamaterial, Axial ratio, Circular polarization etc.

ARTICLE INFORMATION

Author(s): Potnuru Narayanarao, Karunakar Godi;
Received: 29/01/2026; **Accepted**: 05/05/2026; **Published**: 25/06/2026;
E- ISSN: 2347-470X;
Paper Id: IJEER260105;
Citation: 10.37391/ijeer.140215
Webpage-link:
https://ijeer.forexjournal.co.in/archive/volume-14/ijeer-140215.html

Publisher's Note: FOREX Publication stays neutral with regard to jurisdictional claims in Published maps and institutional affiliations.

1. INTRODUCTION

Circular Polarization (CP) antennas have attracted substantial interest in modern high-speed communication systems due to several advantages over linearly polarized (LP) antennas [1]. CP microstrip antennas have gained significant attention in modern wireless communication systems due to their ability to mitigate polarization mismatch, reduce multipath fading, and enhance signal reliability. In recent years, extensive research has been carried out to realize compact, high-performance dual-band CP antennas using various design techniques. CP waves exhibit reduced sensitivity to polarization mismatch and misalignment between transmitting and receiving antennas, improved resilience to multipath fading and enhanced penetration through adverse weather conditions [4]. Consequently, CP antennas have been widely used in global navigation satellite systems (GNSS) [7], GPS [8], IRNSS [9], satellite communication links [10], wireless sensor networks [11], wireless power transfer [12] and radio frequency identification systems for several years [13].

A compact dual-band CP antenna for ISM and vehicular communication applications was reported in [14] where patch shaping and feed optimization were employed to achieve circular polarization at 2.5 GHz and 6 GHz. Although the design demonstrated improved gain performance, it involved relatively complex geometry. Similarly, [15] proposed a dual-band CP antenna for UAV applications using multi-slot and stub loading techniques, achieving enhanced axial ratio bandwidth. However, the design complexity increases due to multiple perturbation elements.

Meta surface and metamaterial-based antennas have also been widely explored for performance enhancement. In [16], a meta surface-based CP MIMO antenna was introduced that significantly improved bandwidth and isolation characteristics. Despite these advantages, meta surface-based designs typically require multilayer configurations, increasing fabrication complexity and cost. In another study, dual-band CP operation was achieved using hybrid feeding techniques such as 90° couplers [17], which provided wider axial ratio bandwidth but at the expense of increased circuit complexity.

Reconfigurable CP antennas have also been investigated to enhance functionality. A dual-band polarization-reconfigurable antenna using PIN diodes was presented in [18-19], enabling dynamic switching between polarization states. While such designs offer flexibility, they require biasing circuits and introduce additional losses. Furthermore, high-gain CP antennas using sequential rotation arrays have been reported in [20], where multiple elements and feeding networks were employed to achieve improved radiation performance. However, these array-based designs significantly increase the antenna size and structural complexity.

FOREX Publication
Open Access | Rapid and quality publishing
International Journal of Electrical and Electronics Research (IJEER)
Research Article | Volume 14, Issue 02| Pages 381-388 | e-ISSN: 2347-470X

In addition, dual-band CP antennas for space and satellite applications have been developed, such as the CubeSat antenna reported in [21], which achieved high gain and stable CP performance. Nevertheless, such designs are generally not suitable for low-cost terrestrial applications due to their stringent design and fabrication requirements.

The metamaterials have a promising platform for advanced polarization control owing to their unconventional electromagnetic properties, enabling functionalities such as cross polarization conversion, conversion between right-hand and left-hand CPs and asymmetric transmission. The work focuses on the design of the truncated corners based square patch along with the slot at the center to achieve circular polarization, the gain is enhanced using the metamaterials.

The paper is organized as follows: *Section 2* explains the antenna design with square ring resonators (SRR) metamaterials. *Section 3* describes parameters affecting circular polarization and return loss using simulations. The fabrication and experimental validation of the work is presented in *section 4*, followed by conclusions in *section 5*.

2. ANTENNA DESIGN WITH SRR METAMATERIAL

A compact dual-band CP microstrip patch antenna was systematically developed using an incremental design approach. The design methodology for the proposed antenna structure is presented in the *figure 1*.

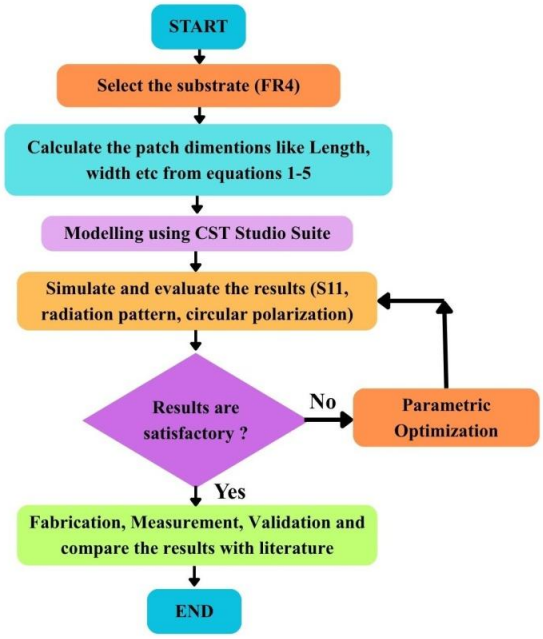

Figure 1. Design methodology for the proposed antenna design

The microstrip patch dimensions are calcualted using the below equaitons. The patch width is calculated using the formula

$$W = \frac{c}{2f_r}\sqrt{\frac{2}{\varepsilon_r+1}} \quad (1)$$

Where ε_r is the dielectric constant of the microwave substrate. The effective dielectric constant of the material is

$$\varepsilon_{reff} = \frac{\varepsilon_r+1}{2} + \frac{\varepsilon_r-1}{2}\left[1+12\frac{h}{W}\right]^{\frac{-1}{2}}, \frac{W}{h} > 1 \quad (2)$$

The infinitsimal length of the dimensions are

$$\frac{\Delta L}{h} = 0.412\frac{(\varepsilon_{reff}+0.3)\left(\frac{W}{h}+0.264\right)}{(\varepsilon_{reff}-0.258)\left(\frac{W}{h}+0.8\right)} \quad (3)$$

The patch length is

$$L = \frac{c}{2f_r\sqrt{\varepsilon_{reff}}} - 2\Delta L \quad (4)$$

The SRR resonance is

$$f_0 = \frac{1}{2\pi\sqrt{LC}} \quad (5)$$

The first structure is a simple square patch antenna with a dimension of 50x50x1.6 mm^{3}and was thoroughly investigated to the final optimized design and is represented in *figure 2(a)-(c)*. The completed antenna features a radiating top layer with a specifically tailored geometry and a complete ground plane in other side of the substrate as represented in *figure 2(d)*. The finalized structure includes a square patch configured on the top side of the substrate, truncated at opposing corners of the square patch and an etched rectangular slot on the patch. The rectangular slots are extended to two opposite sides of the etched portions. The rectangular etched features both of which play a critical role in tuning and optimization of the operating frequency bands. The proposed SRR-based metamaterial structure is represented in the *figure 2(e)*. The design integrates a 50 Ω line feed and is fitted with an SMA connector at the feed line termination for measurements.

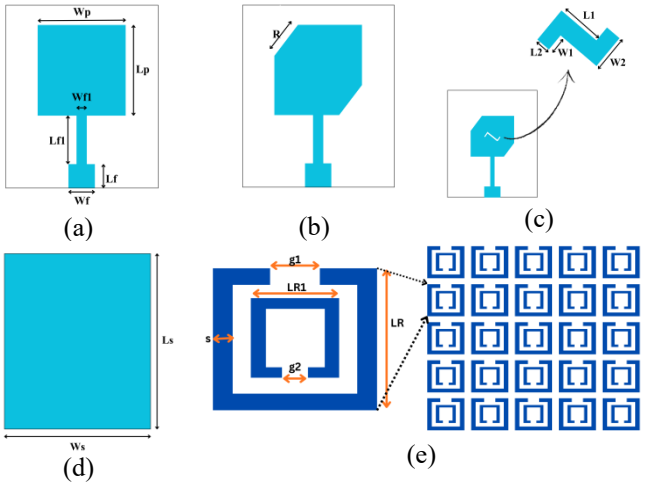

Figure 2. (a) Basic square patch (Design 1) (b) Truncated Square Patch (Design 2) (c) Proposed antenna (d) Ground Plane (e) Proposed antenna with SRR metamaterial

FOREX Publication
Open Access | Rapid and quality publishing
International Journal of Electrical and Electronics Research (IJEER)
Research Article | Volume 14, Issue 02| Pages 381-388 | e-ISSN: 2347-470X

Table 1. SRR based Antenna design parameters

Parameter	Value (mm)	Parameter	Value (mm)
Ls	50	L1	7.5
Lf	3	W1	0.5
Ws	50	L2	0.5
Wf	3	W2	1
Wfl	1.25	LR	3.8
Lfl	12	LR1	2
Wp	30	S	0.5
Lp	30	G	0.5
R	4	G1	0.5

In the design process, successive geometric modifications were applied and started with the basic patch with a square patch, truncated patch edges on the opposite sides, introducing etched rectangular stubs at the centre of the patch with extended edges of the rectangular stubs at the edges of the centre stub. Each iteration's dimensions were refined using commercially available CST Studio Suite software for optimal impedance matching, bandwidth, and polarization characteristics. *Table 1* summarizes the critical design parameters of the final antenna design. This structured evolution ensured that the final configuration offered robust dual-band circular polarization and efficient performance optimized for wireless communications.

3. SIMULATION RESULTS

The SRR metamaterial-based proposed antenna design was modelled and analyzed using a commercially available 3D full-wave electromagnetic (EM) simulation software, CST Studio Suite. The 3D EM software is equipped with an advanced computer-aided design (CAD) interface. The FDTD solver in CST accurately computes all three vector components of the electric (E) and magnetic (H) fields, enabling precise characterization of complex radiating structures. The proposed antenna was configured with appropriate boundary conditions, and an excitation was applied through a wave port positioned at the edge of the feedline. CST utilizes the FDTD solver, offering high numerical accuracy and efficiency for integrated antenna geometries. A fine mesh resolution of 5mm was applied during the simulation and the antenna geometry was tuned and optimized to achieve improved performance. The parameters influencing antenna performance include Lp, R, L1, W1, L2, W2, Wfl and Lfl.

Figure 3 consists of the reflection coefficient parameter of Design 1, Design 2, the proposed antenna and with the SRR metamaterial. From the simulation results, observes that the antenna with SRR metamaterial operates in dual bands, at 2.4 and 4.5 GHz frequencies. The first operating frequency range is from 2.28 - 2.48 GHz with a bandwidth of 180 MHz, and the second operating range of frequencies, from 4.48 to 4.64 GHz, with a bandwidth of 160 MHz. The simulation results confirm that the antenna maintains a return loss below −10 dB across the bands of 2.24-2.48 GHz and 4.48-4.64 GHz. The *x*-axis represents frequency, while the *y*-axis denotes the reflection coefficient in dB.

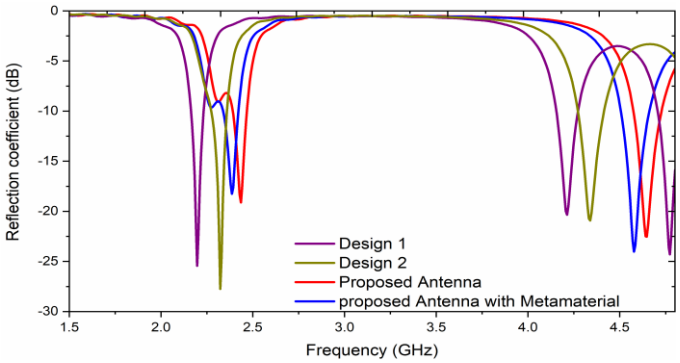

Figure 3. Simulation results of Design 1, Design 2, Proposed antenna and Proposed antenna with SRR metamaterial

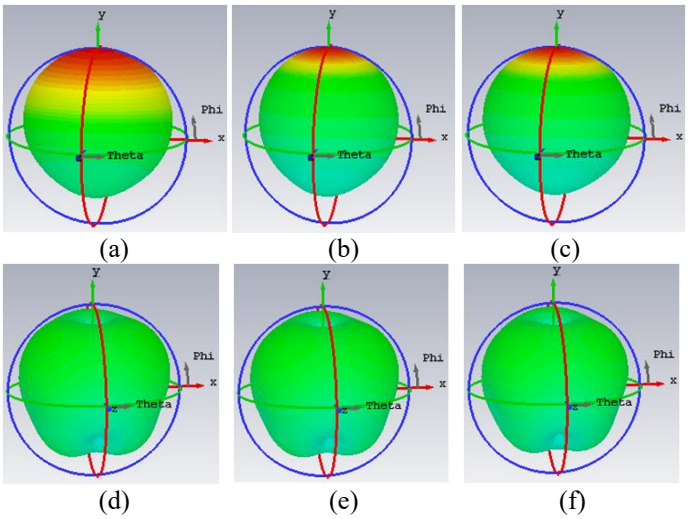

Figure 4. 3D radiation pattern of the Design 1 for the frequencies (a) 2.3 (b) 2.4 (c) 2.45 (d) 4.48 (e) 4.5 (f) 4.6GHz

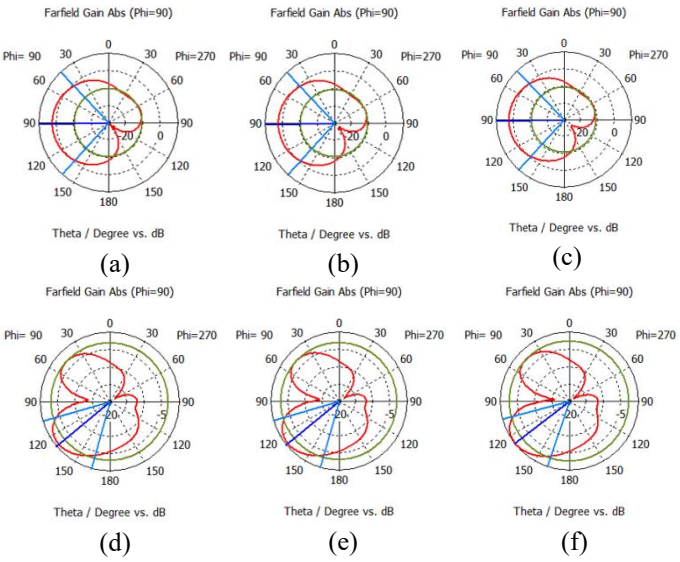

Figure 5. 2D radiation pattern of the Design 1 for the frequencies (a) 2.3 (b) 2.4 (c) 2.45 (d) 4.48 (e) 4.5 (f) 4.6GHz.

FOREX Publication
Open Access | Rapid and quality publishing
International Journal of Electrical and Electronics Research (IJEER)
Research Article | Volume 14, Issue 02| Pages 381-388 | e-ISSN: 2347-470X

The 3D and 2D radiation patterns of the Design 1 is represented in *figure 4* and *figure 5* respectively. The simulated radiation characteristics like Gain and beamwidth of the Design 1 is represented in *table 2*. The 3D radiation pattern of the Design 1 for the frequencies 2.3, 2.4 and 2.45 GHz is illustrated in *figure 4 (a)* to *(c)* and the frequencies 4.48, 4.5 and 4.6 GHz are represented in *figure 4(d)* to *(f)* respectively.

The 2D radiation pattern of the Design 1 for the frequencies 2.3, 2.4 and 2.45 GHz is shown in *figure 5 (a)* to *(c)* and the frequencies 4.48, 4.5 and 4.6 GHz are represented in *figure 5(d)* to *(f)* respectively.

The 3D and 2D radiation patterns of the Design 2 is represented in *figure 6* and *7* respectively. The simulated radiation characteristics like Gain and beamwidth of the Design 2 is represented in *table 2*. The 3D radiation pattern of Design 2 for the frequencies 2.3, 2.4 and 2.45 GHz is illustrated in the *figure 6 (a)* to *(c)* and the frequencies 4.48, 4.5 and 4.6 GHz are represented in *figure 6(d)* to *(f)* respectively.

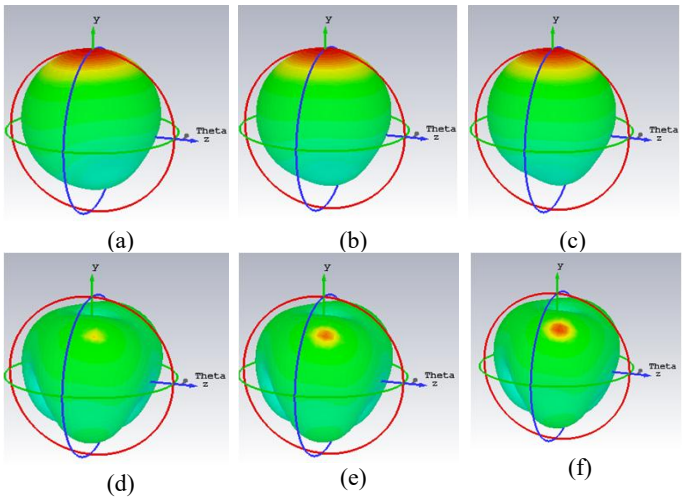

Figure 6. 3D radiation pattern of the Design 2 for the frequencies (a) 2.3 (b) 2.4 (c) 2.45 (d) 4.48 (e) 4.5 (f) 4.6GHz

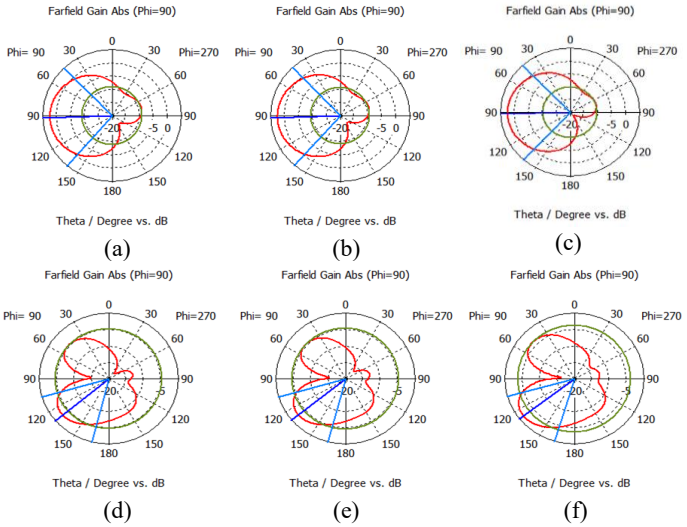

Figure 7. 2D radiation pattern of the Design 2 for the frequencies (a) 2.3 (b) 2.4 (c) 2.45 (d) 4.48 (e) 4.5 (f) 4.6GHz

The 2D radiation pattern of the Design 2 for the frequencies 2.3, 2.4 and 2.45 GHz is shown in *figure 7 (a)* to *(c)* and the frequencies 4.48, 4.5 and 4.6 GHz are represented in *figure 7(d)* to *(f)*, respectively.

The 3D and 2D radiation patterns of the proposed antenna is represented in *figure 8* as well as in *figure 9*. The simulated radiation characteristics like Gain and beamwidth of the proposed antenna is represented in *table 2*. 3D radiation pattern of the proposed antenna at the operating frequencies of 2.4, 2.45 and 2.5 GHz is represented in *figure 8 (a)* to *(c)* and the frequencies 4.48, 4.5 and 4.6 GHz are represented in *figure 8(d)* to *(f)* respectively.

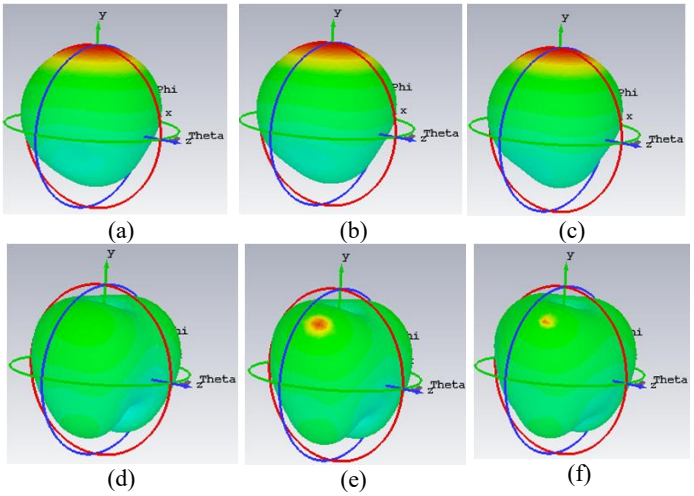

Figure 8. 3D radiation pattern of the proposed antennafor the frequencies (a) 2.3 (b) 2.4 (c) 2.45 (d) 4.48 (e) 4.5 (f) 4.6GHz

The 2D radiation pattern of the proposed antenna for the frequencies 2.3, 2.4 and 2.45 GHz is illustrated in *figure 9 (a)* to *(c)* and the frequencies 4.48, 4.5 and 4.6 GHz are represented in *figure 9 (d)* to *(f)* respectively.

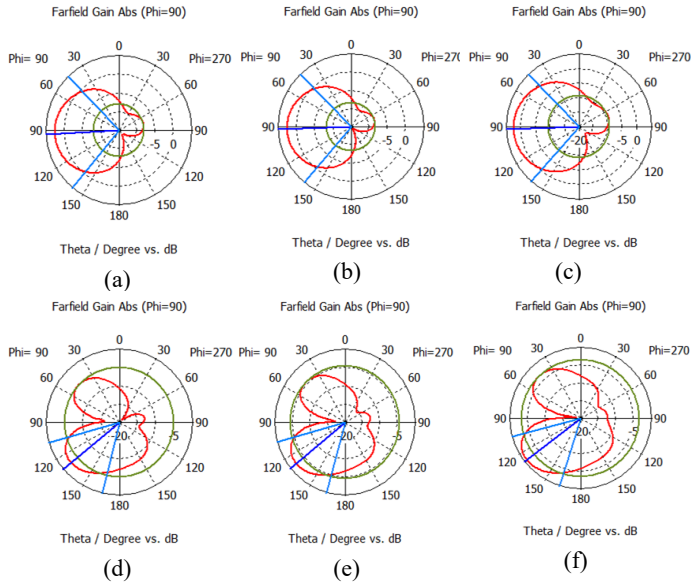

Figure 9. 2D radiation pattern of the proposed antennafor the frequencies (a) 2.3 (b) 2.4 (c) 2.45 (d) 4.48 (e) 4.5 (f) 4.6GHz

FOREX Publication
Open Access | Rapid and quality publishing
International Journal of Electrical and Electronics Research (IJEER)
Research Article | Volume 14, Issue 02| Pages 381-388 | e-ISSN: 2347-470X

The 3D and 2D radiation patterns of the proposed antenna with metamaterial are represented in *figure 10* and *figure 11* respectively. The simulated radiation characteristics like Gain and beamwidth of the proposed antenna with metamaterial is represented in *table 2*. The 3D radiation pattern of the proposed antenna with SRR metamaterial for the frequencies 2.3, 2.4 and 2.45 GHz is shown in *figure 10 (a)* to *(c)* and the frequencies 4.48, 4.5 and 4.6 GHz are represented in *figure 10(d)* to *(f)* respectively.

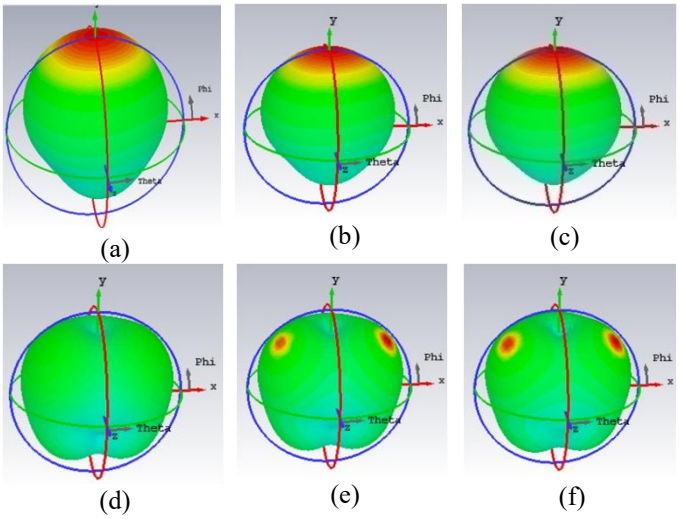

Figure 10. 3D radiation pattern of the proposed antenna with SRR Metamaterialfor the frequencies (a) 2.3 (b) 2.4 (c) 2.45 (d) 4.48 (e) 4.5 (f) 4.6GHz

The 2D radiation pattern of the proposed antenna with SRR metamaterial for the frequencies 2.3, 2.4 and 2.45 GHz is represented in *figure 11 (a)* to *(c)* and the frequencies 4.48, 4.5 and 4.6 GHz are represented in *figure 11 (d)* to *(f)* respectively.

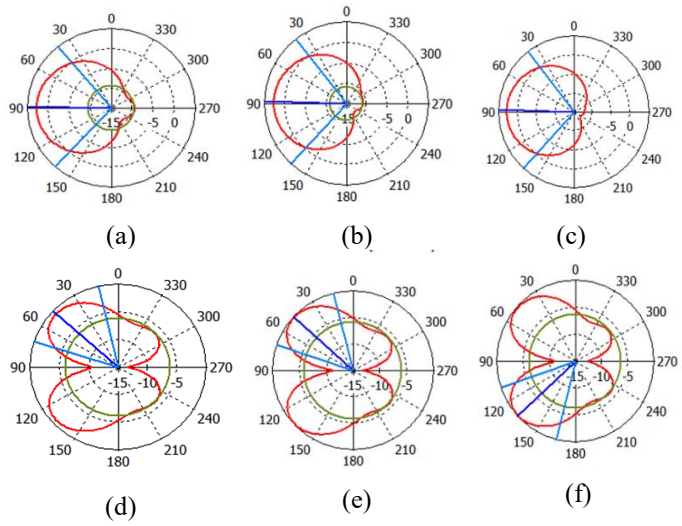

Figure 11. 2D radiation pattern of the proposed antennafor the frequencies (a) 2.3 (b) 2.4 (c) 2.45 (d) 4.48 (e) 4.5 (f) 4.6GHz

CP in microstrip antennas is achieved through the use of truncated corners, which helps current distribution over the patch to enhance the antenna's polarization properties. Among the three antenna geometries analyzed by the inclusion of rectangular slots are effective for reducing the AR to below 3 dB across the operating frequency range. The simulated AR performance of the three antennas over the operating frequencies is tabulated in the Table 3. The proposed antenna and the proposed antenna with metamaterial configuration exhibited AR values are less than 3 dB and indicating CP performance. The simulation results illustrate the effectiveness of the design refinements in satisfying axial ratio criteria for optimal CP and enhancing the work is suitable for wireless communication.

The CP is evaluated using the AR, the AR for Design 1, Design 2, the proposed antenna and the proposed antenna with a metamaterial are represented in *table 3*. Including the truncated corners in the square patch and the rectangular stubs of the proposed antenna design led to significant improvements in terms of AR values of 2.81 dB at 2.4 GHz and 2.6 dB at 4.5 GHz. These outcomes highlight the effectiveness of these design modifications in meeting the AR criteria required for optimal circular polarization performance, thereby increasing the antenna's suitability for wireless applications. The results clearly emphasize that precise tuning of the antenna geometry is crucial for achieving the desired polarization characteristics.

Table 2. Radiation characteristics of the Design 1, Design 2, proposed antenna and proposed antenna with metamaterial.

Freq (GHz)	Design 1		Design 2		Proposed antenna		Proposed antenna with metamaterial	
	G	BW	G	BW	G	BW	G	BW
2.3	1.93	95.3	2.16	95.8	2.41	96.1	2.6	98.5
2.4	1.97	94.7	2.33	92.0	2.39	95.8	2.54	99.6
2.45	2.18	94.2	2.25	91.0	2.26	95.0	2.67	100.0
4.48	1.06	58.6	2.88	59.9	2.92	60.3	3.2	58.6
4.5	0.83	57.8	2.66	59.3	2.23	59.1	2.6	57.3
4.6	0.31	56.1	1.66	57.8	0.935	57.6	1.8	57.0

Where, G - Gain (dBi); BW- Beamwidth (degrees)

Table 3. Axial Ratio of the Design 1, Design 2, proposed antenna and proposed antenna with SRR metamaterial

Freq (GHz)	Design 1	Design 2	Proposed antenna	Proposed antenna with metamaterial
2.3	40	16.05	2.94	2.90
2.4	40	15.31	2.85	2.71
2.45	40	14.81	2.73	2.61
4.48	40	14.07	2.72	2.68
4.5	40	13.94	2.67	2.61
4.6	40	18.34	2.31	2.23

The combined integration of truncated corners, rectangular slot loading, and SRR-based metamaterial structure to achieve dual-band circular polarization with improved axial ratio and stable gain using a simple single-layer configuration.

FOREX Publication
Open Access | Rapid and quality publishing
International Journal of Electrical and Electronics Research (IJEER)
Research Article | Volume 14, Issue 02| Pages 381-388 | e-ISSN: 2347-470X

4. MEASURED RESULTS

The fabricated prototypes of the proposed antenna and 5 X 5 SRR metamaterial structure are represented in *figure 12(a)* and *12(c)*, respectively. The proposed antenna as well as metamaterial, is developed using photolithography techniques. The measurements are carried out using Keysight Vector Network Analyzer (VNA), and the corresponding return loss is represented in *figure 13*. The simulated results exhibit strong agreement with the corresponding experimental measurements.

(a) (b) (c)

Figure 12. Fabricated prototypes of proposed antenna (a) top of the patch (b) bottom ground plane (c) metamaterial structure

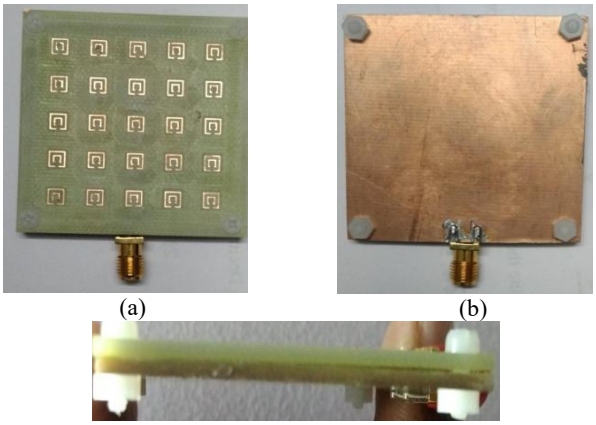

(a) (b) (c)

Figure 13. Fabricated prototypes of proposed antenna with metamaterial (a) top view (b) bottom view (c) side view

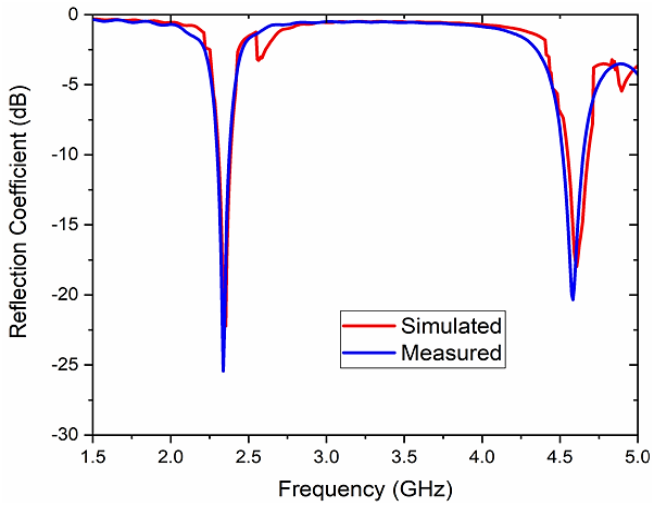

Figure 14. Simulated vs measured parameter of reflection coefficient of proposed antenna with metamaterial

The measurement setup of the radiation pattern in an anechoic chamber of the proposed antenna with metamaterial is represented in *figure 15*. The *E* and *H* field radiation pattern for the frequencies 2.4 and 4.5 GHz are represented in *figure 16(a)* and *(b)* respectively.

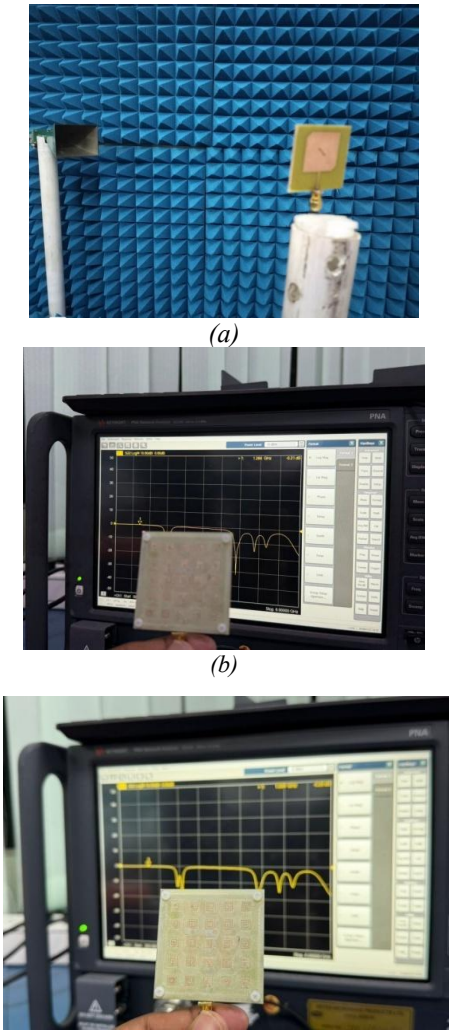

(a) *(b)* (c)

Figure 15. Radiation pattern measurement setup in anechoic chamber

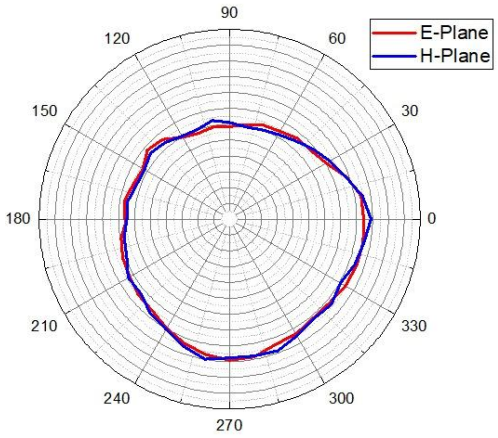

(a)

FOREX Publication
Open Access | Rapid and quality publishing
International Journal of Electrical and Electronics Research (IJEER)
Research Article | Volume 14, Issue 02| Pages 381-388 | e-ISSN: 2347-470X

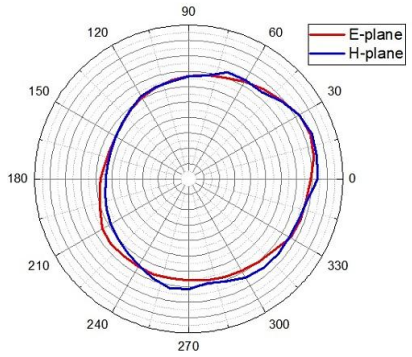

(b)

Figure 16. Measured radiation pattern of the proposed antenna with metamaterial (a) 2.4 GHz and (b) 4.5 GHz

The radiation characteristics of the proposed antenna with a metamaterial is represented in *table 4*. The measured radiation characteristics of Beamwidth, Gain and AR are giving good matching with the simulation results.

Table 4. Measured Radiation characteristics of the proposed antenna with metamaterial

Freq (GHz)	Beamwidth (degrees)	Gain (dB)	AR (dB)
2.4	98.2	2.61	2.75
4.5	57	2.8	2.5

The proposed antenna achieves dual-band CP with a simple geometry, unlike existing works that rely on complex feeding or multilayer structures. The comparison of the proposed antenna with existing literature is tabulated in *table 5*.

Table 5. Comparison of Table of the proposed work with literature

Ref	Overall size (mm^3)	Antenna Type	Frequency (GHz)	Bandwidth (GHz)	Gain (dBi)	AR (dB)	Key feature	Comparison with Proposed work
[14]	62 x 62 x 1.6	Modified Circular Patch	2.5, 6	-	1.8 dBi @2.5 GHz, 3.8 dBi @6 GHz	< 3 dB	Industrial, scientific and medical (ISM) and Vehicle to everything (V2x) communications systems.	Higher Gain and complex structure.
[22]	48.7 x 42.1 x 1.016	Monopole rectangular patch	2.45, 5.8	0.86 and 1.5	1.64 and 2.65 @lower CP bands	< 3 dB	Wearable devices.	Indirectly coupled parasitic patch structure.
[15]	40 x 40 x 1.6	Etched circular patch antenna.	2.4, 5	0.129, 0.47	5.01 @2.4 and 5.27 @ 5 GHz	< 3 dB	Unmanned Aerial Vehicle applications	Multiple slots and stubs.
[16]	49.2 x 32.8 x 1.52	Truncated corner square patch antenna	5-5.6	0.6	4.4 dBi	< 3 dB	C-band WLAN applications and satellite communications	MIMO antenna with meta surfaces
[23]	60 x 40 x 1.58	CPW based split ring resonator antenna	2.45	~0.4	2.1	< 3 dB	Wireless harvesting energy.	Low input RF power with wide operating rectenna applications.
Proposed work	50 x 50 x 1.6	Square patch with impedance matching network	2.4, 4.5	0.2, 0.18	2.62, 2.8	< 3 dB	WLAN applications	Square patch antenna with a slot at the center.

5. CONCLUSION

The proposed antenna with SRR metamaterial demonstrates excellent performance in terms of gain and AR and is highly suitable for wireless applications. The integration of a proposed antenna with SRR metamaterial enhances the antenna's operational characteristics and achieves a simulated bandwidth of 0.18 GHz and 0.16 GHz, and a measured bandwidth of approximately 0.2 and 0.18 GHz at 2.4 GHz and 4.5 GHz, respectively. The achieved peak gain of 2.62 dB and 2.8 dB at 2.4 and 4.5 GHz, respectively. The close agreement between simulation and experimental results validates the reliability of the design approach and the precision of the fabrication process. The compact size and efficiency in performance make the antenna well-suited for commercial wireless applications requiring high radiation efficiency as well as circular polarization. Thefuture work of this work includes gain enhancement using arrays, as well as reconfigurable circular polarization and integration with MIMO systems.

REFERENCES

[1] M. Moharana and B. Dwivedy, "Circularly Polarized Planar Antennas with Enhanced Characteristics for Contemporary Wireless Communication Use Cases: A Review," in IEEE Access, vol. 12, pp. 134594-134613, 2024, doi: 10.1109/ACCESS.2024.3415483.

[2] B. Dwivedy and S. K. Behera, "A square-shaped microstrip antenna with frequency and circular-polarization reconfigurability: An approach [antenna applications corner]," IEEE Antennas Propag. Mag., vol. 62, no. 4, pp. 107–115, Aug. 2020.

[3] Y.-D. Yan, Y.-C. Jiao, H.-T. Cheng, and C. Zhang, "A low-profile dual-circularly polarized wide-axial-ratio-beamwidth slot patch antenna with six-port feeding network," IEEE Antennas Wireless Propag. Lett., vol. 20, pp. 2486–2490, 2021.

[4] Rajni, and A. Marwaha, "An accurate approach of mathematical modeling of srr and sr for metamaterials," Journal of Engineering Science and Technology Review, Vol. 9, 82–86, 2016. [Online]. Available: https://api.semanticscholar.org/CorpusID: 117262210

[5] Liu, W., Z. N. Chen, and X. Qing, "Low-profile broadband antennas using metamaterial-mushroom structures (invited)," in 2015 IEEE International Conference on Computational Electromagnetics, 33–34, 2015

[6] Esmail, B. A. F. and S. Koziel, "Design and optimization of metamaterial-based highly isolated mimo antenna with high gain and beam tilting ability for 5g millimeter wave applications," Scientific Reports, Vol. 14, No. 1, 3203, Feb 2024. [Online]. Available: https://doi.org/10.1038/s41598-024-53723-8

[7] Esmail, K. S., Bashar AF, "Design and optimization of metamaterial-based dual-band 28/38 ghz 5g mimo antenna with modified ground for isolation and bandwidth improvement," IEEE Antennas and Wireless Propagation Letters, Vol. 22, No. 5, 1069–1073, 2023

[8] Milias, C., R. Andersen, P. Lazaridis, Z. Zaharis, B. Muhammad, J. Kristensen, A. Mihovska, and D. Hermansen, "Metamaterial-inspired antennas: A review of the state of the art and future design challenges," IEEE Access, Vol. 9, 89 846–89 865, Jun. 2021, publisher Copyright: CCBY Copyright: Copyright 2021 Elsevier B.V., All rights reserved.

[9] Reddy, M. H., D. Sheela, V. K. Parbot, and A. Sharma, "A compact metamaterial inspired uwb-mimo fractal antenna with reduced mutual coupling," Microsystem Technologies, Vol. 27, No. 5, 1971–1983, May 2021. [Online]. Available: https://doi.org/10.1007/s00542-020-05024-z

[10] Ameen, M. and R. K. Chaudhary, "Isolation enhancement of metamaterial-inspired two-port mimo antenna using hybrid techniques," IEEE Transactions on Circuits and Systems II: Express Briefs, Vol. 70, No. 6, 1966–1970, 2023.

[11] Potnuru, N. and K. Godi, "Design of a high-gain wideband co-planar waveguide antenna for wireless communications using metamaterial techniques," Engineering, Technology &; Applied Science Research, Vol. 15, No. 4, 25257–25262, Aug. 2025. [Online]. Available: https://etasr.com/index.php/ETASR/article/view/11565

[12] Abdalla, M. A., Z. Hu, and C. Muvianto, "Analysis and design of a triple band metamaterial simplified crlh cells loaded monopole antenna," International Journal of Microwave and Wireless Technologies, Vol. 9, No. 4, 903–913, 2017.

[13] Zhu, J.-X., P. Bai, and J.-F. Wang, "Ultrasmall dual-band metamaterial antennas based on asymmetrical hybrid resonators," International Journal of Antennas and Propagation, Vol. 2016, No. 1, 7019268, 2016. [Online]. Available: https://onlinelibrary.wiley.com/doi/abs/10.1155/2016/7019268

[14] E. D. Kanmani Ruby, S. K. Palanisamy, and O. I. Khalaf, "Compact circularly polarized dual-band antenna for ISM and vehicular communication systems," Scientific Reports, vol. 15, 2025.

[15] A. S. Almehmadi and R. W. Aldhaheri, "Dual-band circularly polarized microstrip antenna for UAV applications," Applied Sciences, vol. 15, no. 4, 2025.

[16] H.-H. Tran, T. T. Nguyen, and J. H. Lee, "A compact circularly polarized MIMO antenna using metasurface for wireless applications," Electronics, vol. 12, no. 2, pp. 384, 2023.

[17] M. A. Abdalla, Z. Hu, and C. Muvianto, "Circularly polarized antenna using hybrid coupler for wide axial ratio bandwidth," Applied Sciences, vol. 14, no. 24, 2024.

[18] M. Rezvani and Y. Zehforoosh, "Dual-band dual-sense circularly polarized patch antenna using hybrid coupling," AEU - International Journal of Electronics and Communications, vol. 184, 2024.

[19] M. Fathipour and L. Asadpor, "Dual-band polarization reconfigurable microstrip antenna using PIN diodes," AEU - International Journal of Electronics and Communications, vol. 171, 2023.

[20] G. Dai, X. Xu, and X. Ding, "Dual-band dual circularly polarized patch antenna using sequential rotation technique," AEU - International Journal of Electronics and Communications, vol. 175, 2024.

[21] J. Huang, K. Boyle, and R. J. Langley, "Dual-band circularly polarized microstrip antenna for CubeSat applications," Acta Astronautica, vol. 203, pp. 1–10, 2023.

[22] Y. Dong, H. Lu, and X. Chen, "A novel dual-band circularly polarized wearable antenna," *Micromachines*, vol. 15, no. 5, Art. no. 588, 2024, doi: 10.3390/mi15050588.

[23] M. Bajtaoui, O. El Mrabet, M. A. Ennasar, and M. Khalladi, "A novel circularly polarized rectenna with wide ranges of loads for wireless energy harvesting," *Progress In Electromagnetics Research M*, vol. 106, pp. 35–46, 2021, doi: 10.2528/PIERM21092107.